High level expression of expanded full-length ataxin-3 in vitro causes cell death and formation of intranuclear inclusions in neuronal cells

Evert, B O

DOI: https://doi.org/10.1093/hmg/8.7.1169

 Human Molecular Genetics, 1999, Vol. 8, No. 7 **1169–1176**

ARTICLE

High level expression of expanded full-length ataxin-3 *in vitro* causes cell death and formation of intranuclear inclusions in neuronal cells

Bernd O. Evert+, Ullrich Wüllner[1], Jörg B. Schulz, Michael Weller, Peter Groscurth[2], Yvon Trottier[3], Alexis Brice[4] and Thomas Klockgether[1]

Department of Neurology, University of Tübingen, 72076 Tübingen, Germany, [1]Department of Neurology, University of Bonn, 53105 Bonn, Germany, [2]Department of Anatomy, University of Zürich, 8057 Zürich, Switzerland, [3]Institut de Génétique et de Biologie Moléculaire et Cellulaire (IGBMC), 67404 Illkirch Cédex, France and [4]Hôpital de la Salpêtrière, 75651 Paris Cédex 13, France

Received March 2, 1999; Revised and Accepted April 19, 1999

Spinocerebellar ataxia type 3 (SCA3) is caused by a CAG/polyglutamine repeat expansion in the *SCA3* gene. To analyse the pathogenic mechanisms in SCA3, we have generated ataxin-3-expressing rat mesencephalic CSM14.1 cells. In these cells, a post-mitotic neuronal phenotype is induced by temperature shift. The isolated stable cell lines provided high level expression of non-expanded (Q23) or expanded (Q70) human full-length ataxin-3. CSM14.1 cells expressing the expanded full-length ataxin-3 developed nuclear inclusion bodies, strong indentations of the nuclear envelope and cytoplasmic vacuolation. These ultrastructural alterations were present prior to a significantly decreased viability of neuronally differentiated cells expressing expanded ataxin-3. The observed spontaneous cell death did not correlate with formation of intranuclear inclusions and was not apoptotic by ultrastructural analysis. No increased susceptibility to staurosporine-induced apoptosis was found for the expanded or non-expanded ataxin-3-expressing cell lines. These data show that high level expression of expanded full-length ataxin-3 in a neuron-like cell line generates ultrastructural alterations of SCA3 pathogenesis and results in increased spontaneous non-apoptotic cell death.

INTRODUCTION

Spinocerebellar ataxia type 3 (SCA3), also known as Machado–Joseph disease (MJD), is an autosomal dominantly inherited neurological disorder characterized by neuronal loss and gliosis in the dentate nucleus, vestibular nuclei, spinocerebellar tracts, substantia nigra and other nuclei of the basal ganglia (1,2). SCA3/MJD belongs to a group of neurodegenerative diseases that are caused by unstable expansions of CAG trinucleotide repeats encoding polyglutamine tracts in the respective proteins. Currently, this class of disorders includes Huntington's disease (HD), dentatorubralpallidoluysian atrophy (DRPLA), spinal and bulbar muscular atrophy (SBMA) and spinocerebellar ataxia types 1–3, 6 and 7 (3–8). The coding regions of the genes associated with these disorders do not share homology except for the highly polymorphic CAG tract.

The CAG/glutamine repeat of the *SCA3* gene is near the C-terminus. In normal individuals, the repeat length varies between 12 and 37 trinucleotides whereas SCA3 patients have alleles with 61–84 repeat units. As in other trinucleotide repeat disorders, there is an inverse correlation between the CAG repeat length and the age of onset (9,10). The *SCA3* gene encodes ataxin-3, an intracellular protein of unknown function with a predicted molecular weight of 42 kDa, depending on the number of CAG trinucleotides (9,11). Ataxin-3 is a cytoplasmic protein expressed ubiquitously throughout the body. Thus, the regional distribution of ataxin-3 expression does not match the sites of pathology in SCA3 (12,13).

The molecular mechanisms by which polyglutamine expansions cause neurodegeneration remain unclear. Experimental results from several laboratories suggest that expanded polyglutamine may adopt a pathological conformation and engage in inappropriate protein–protein interactions, including intranuclear aggregation of proteins (14–20). Intracellular aggregates of ataxin-3 have been reported only in the presence of an expanded polyglutamine tract, suggesting that this interaction is determined by glutamine length (15). Furthermore, the intranuclear aggregates are ubiquitinated, suggesting a specific proteolytic pathway for immediate degradation of misfolded proteins. Thus, cleavage of an expanded ataxin-3 may liberate a toxic polyglutamine-containing fragment that translocates to the nucleus via polyglutamine-containing transcription factors

+To whom correspondence should be addressed. Tel: +49 228 287 6130; Fax: +49 228 287 5024; Email: b.evert@uni-bonn.de

and forms intranuclear aggregates, thereby also recruiting physiological ataxin-3 in a dominant-negative manner (15,21).

Several transgenic models employing protein fragments with an expanded glutamine repeat resulted in progressive neurodegenerative phenotypes (14,16,22–26). In mice transgenic for exon 1 of an expanded human *HD* gene, pronounced neuronal intranuclear inclusions are observed prior to the development of a neurological phenotype (16). Similarly, transgenic mice expressing a truncated *SCA3* cDNA develop ataxia and cerebellar atrophy (14). In contrast, mice transgenic for a full-length expanded ataxin-3 protein do not demonstrate any neurological phenotype at 23 weeks of age (14).

Recent studies using transiently transfected cells with different sized *HD* or truncated *SCA3* cDNA constructs with expanded CAG repeats have shown formation of intracellular aggregates that correlates with an increased susceptibility to apoptotic cell death (14,15,27–29). In contrast, none of the *in vivo* or *in vitro* models for SCA3 demonstrated an increased susceptibility to cell death resulting from expression of an expanded full-length ataxin-3 protein.

We have established a cellular model for SCA3 in the rat mesencephalic dopaminergic cell line CSM14.1. The CSM14.1 cell line was originally derived from a primary fetal rat mesencephalic cell culture immortalized using the temperature-sensitive SV40 large T antigen (30). This cell line proliferates at the permissive temperature (33°C) and differentiates to a post-mitotic state at the non-permissive temperature (39°C). Different clonal cell lines stably expressing the human *SCA3* cDNA with either a non-expanded or an expanded CAG tract, containing 23 or 70 repeat units, were generated under the transcriptional control of a tetracycline-responsive promoter (31). The established ataxin-3-expressing cell lines provide high level expression of human ataxin-3 variants and allow a study of the effects of long-term ataxin-3 expression. Here, we show that CSM14.1 cells expressing the expanded full-length ataxin-3 protein develop nuclear inclusion bodies and indentations of the nuclear envelope and undergo spontaneous non-apoptotic cell death.

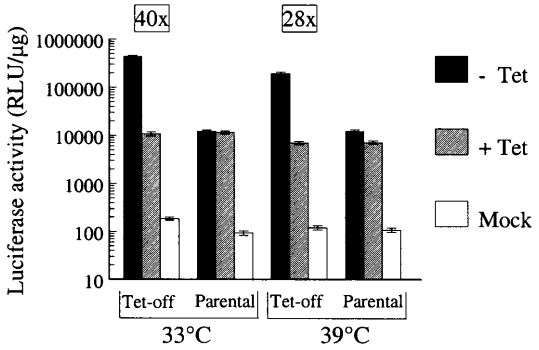

Figure 1. Reporter gene assays of the isolated Tet-off CSM14.1 cell line. Cells of the isolated Tet-off cell line and of the parental cell line were transiently transfected with the tTA-dependent luciferase reporter gene (pUHC13-3) in the absence (–Tet) or presence (+Tet) of tetracycline (1 µg/ml) either at the permissive (33°C) or the non-permissive (39°C) temperature and luciferase activities were measured after 48 h. Levels of induction of luciferase gene expression at 33 and 39°C for the isolated Tet-off cell line are shown in boxes. Mock transfections were performed in the absence of tetracycline using the empty response plasmid pUHD10-3 lacking the luciferase gene. Values represent averages from three independent experiments ± SD.

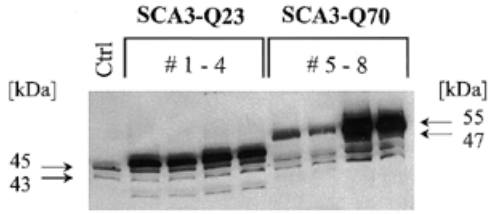

Figure 2. Characterization of the recombinant non-expanded and expanded human ataxin-3 proteins. Cells of stably transfected and selected clonal lines (1–8) were incubated at 33°C in the absence of tetracycline. Lysates were prepared after 48 h and 50 µg protein was analysed for ataxin-3 expression by western blotting using the anti-ataxin-3 antibody 1H9. Clonal lines 1–4 stably transfected with the non-expanded *SCA3* cDNA construct (*SCA3*-Q23) generated an immunoreactive protein of ~47 kDa, whereas clonal lines 5–8 stably transfected with the expanded *SCA3* cDNA construct (*SCA3*-Q70) expressed an immunoreactive protein of ~55 kDa (arrows, right). Both heterologous human ataxin-3 variants were clearly distinct from the endogenous rat ataxin-3 protein (arrows, left) expressed in the mock-transfected control cell line (Ctrl).

RESULTS

Stable cell lines expressing variants of human ataxin-3

The cellular model for SCA3 was established using the Tet-off gene expression system (31). After stable integration of the tetracycline-responsive transcriptional activator (tTA) in the mesencephalic CSM14.1 cell line, the subclone with the highest tetracycline-dependent induction was selected. To characterize the temperature- and tetracycline-dependent regulation of the isolated Tet-off CSM14.1 cell line, reporter gene assays were performed with tTA-dependent luciferase. The isolated Tet-off cell line exhibited a 40-fold induction of luciferase gene expression at 33°C and a 28-fold induction at 39°C (Fig. 1). In the presence of tetracycline, a residual tetracycline-insensitive expression of luciferase was observed that was not present in mock-transfected controls of each cell line (Fig. 1).

Subsequently, the isolated Tet-off cell line was used to generate double stably transfected CSM14.1 cell lines expressing human ataxin-3 protein with a non-expanded repeat (*SCA3*-Q23) or an expanded repeat (*SCA3*-Q70). Western blot analysis of individual cell clones (Fig. 2) showed strong expression of human ataxin-3 protein of appropriate sizes of 47 and 55 kDa for non-expanded ataxin-3 (*SCA3*-Q23) and expanded ataxin-3 (*SCA3*-Q70), respectively. These sizes were consistent with the number of CAG repeats present within the *SCA3* cDNA expression constructs. Endogenous rat ataxin-3 with two weak immunoreactive bands of ~43 and 45 kDa was also detected by the ataxin-3 specific antibody 1H9 (32) in lysates of the isolated human ataxin-3-expressing clonal cell lines and in the stable mock-transfected control cell line (Fig. 2).

To analyse the time course of ataxin-3 expression after tetracycline withdrawal, cells were collected after 7, 14 and 21 days of incubation without and with tetracycline (1 µg/ml). The protein levels of the recombinant ataxin-3 variants increased with time from day 7 to 21 (Fig. 3). Maintaining tetracycline (1 µg/ml) in the medium prevented the increase in the signal intensity of the 47 and 55 kDa immunoreactive bands seen in the absence of tetracycline, but did not eliminate ataxin-3 expression. Thus, considerable tetracycline-insensitive expression of ataxin-3 occurred in the isolated ataxin-3-expressing cell lines. Increasing

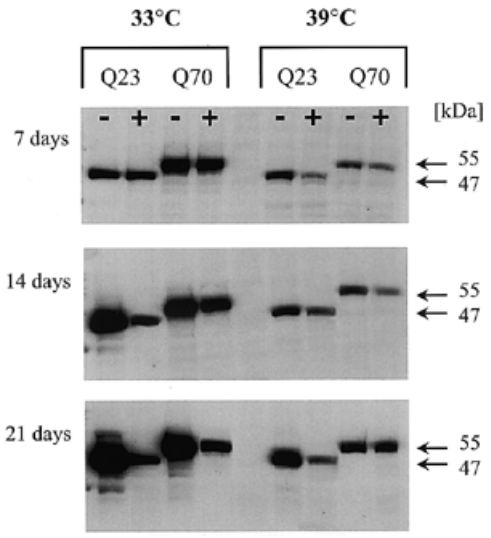

Figure 3. Time course of ataxin-3 expression. Western blot analysis of recombinant human full-length ataxin-3 protein expressed in two clonal cell lines after 7, 14 and 21 days at the permissive (33°C) and non-permissive (39°C) temperatures. Lysates were prepared after continued induction (–) or sustained suppression (+) from cells expressing the human non-expanded (Q23) or expanded (Q70) ataxin-3 isoforms at the indicated time points and 20 µg protein were analysed by western blotting using the anti-ataxin-3 antibody 1H9. Note that chemiluminescent detection of immunoblots was performed simultaneously and demonstrated a continuous increase in heterologous expression over time. The ataxin-3 immunoreactive bands of 47 and 55 kDa corresponding to non-expanded and expanded human ataxin-3 protein, respectively, are indicated on the right (arrows).

tetracycline concentrations (5, 10, 15 and 20 µg/ml) did not further inhibit expression but killed a substantial portion of the cells above 10 µg/ml tetracycline after 48 h of exposure (data not shown). Expression of ataxin-3 at the permissive temperature (33°C) was higher than at the non-permissive temperature (39°C), although the increase in ataxin-3 expression after tetracycline withdrawal was comparable (Fig. 3). Interestingly, no proteolytic fragments of the recombinant ataxin-3 protein variants were detected on immunoblots with antibody 1H9 during the period examined. Thus, the selected transgenic cell lines provided high level expression of full-length human ataxin-3 with a non-expanded and an expanded polyglutamine stretch. They were further used in the absence of tetracycline to study the biological effects in neuronal cells resulting from expression of the recombinant proteins.

Immunocytochemical detection of recombinant ataxin-3

The subcellular localization of recombinant ataxin-3 in the established cell lines was analysed by immunocytochemistry using the anti-ataxin-3 antibody 1H9 (32). As expected, all cells of the transgenic lines that stably overexpressed either the non-expanded (Fig. 4c and d) or the expanded full-length ataxin-3 (Fig. 4e and f) exhibited strong ataxin-3-positive staining. Both recombinant ataxin-3 protein variants were not only present in the cytoplasm but also in the nuclei (Fig 4d and f). In contrast, cells of the mock-transfected control cell line exhibited only a weak cytoplasmic and nuclear staining representing the endogenous rat ataxin-3 (Fig. 4a and b).

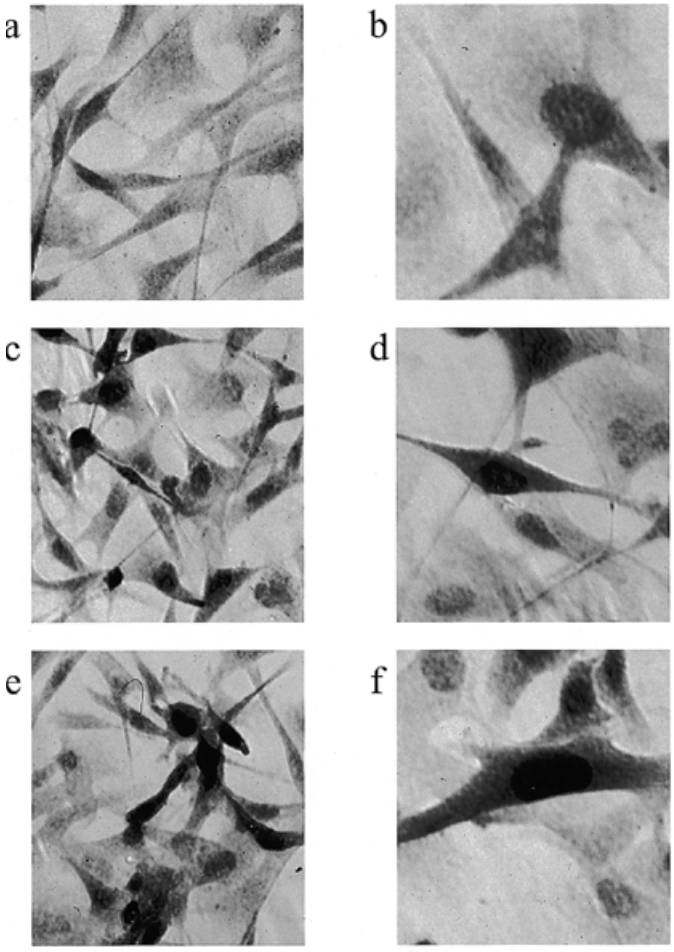

Figure 4. Immunoreactivity of stable transfected cells expressing non-expanded and expanded human full-length ataxin-3. CSM14.1 cells expressing non-expanded and expanded ataxin-3, as well as the mock-transfected control cell line, were cultured for 3 days on culture slides without tetracycline at 33°C and immunostained with the anti-ataxin-3 antibody 1H9. (**a** and **b**) In mock-transfected control cells a weak cytoplasmic and nuclear distribution of endogenous rat ataxin-3 was present. Cells expressing (**c** and **d**) recombinant non-expanded ataxin-3 or (**e** and **f**) expanded ataxin-3 showed cytoplasmic and strong nuclear staining. Magnifications: (a, c and e) 400×; (b, d and f) 630×.

Spontaneous cell death of cell lines expressing expanded ataxin-3

To address the question whether the expanded form of ataxin-3 affects the viability of the cells, long-term incubations up to 26 days were performed at both temperatures and viability was assessed by MTT assays at different time points. All selected cell lines exhibited continuous cell growth at the permissive temperature and reached confluence after 26 days (Fig. 5a). At the non-permissive temperature, cells stopped dividing after 8 days of incubation (Fig. 5b). The viability of *SCA3*-Q70 clonal cell lines decreased significantly at 20 and 26 days incubation compared with the respective values at 8 days, whereas *SCA3*-Q23 clonal cell lines and the mock-transfected control cell line survived until day 26 without significant loss of viability (Fig. 5b). Thus, the *SCA3*-Q70 clonal cell lines exhibited a significant loss of viability only in the neuron-like state at 39°C.

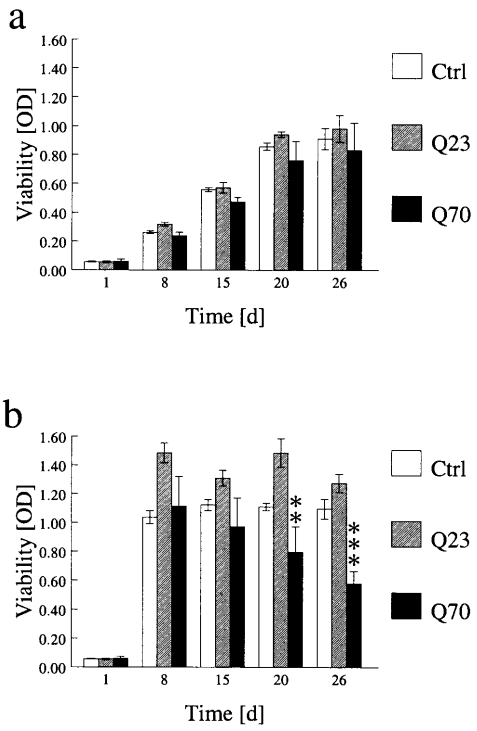

Figure 5. Temperature-dependent cell proliferation and viability of clonal cell lines stably expressing recombinant human full-length ataxin-3 over a time course of 26 days. Cells were cultured in the absence of tetracycline at 33 (**a**) and 39°C (**b**) for the indicated periods of time. Viability was measured by their ability to reduce MTT. At 33°C the clonal cell lines of *SCA3*-Q23 (Q23), *SCA3*-Q70 (Q70) and the mock-transfected control cell line (Ctrl) exhibited continuous growth, whereas they stopped dividing after 8 days at 39°C. A significant decrease in viable cells of neuronally differentiated cells expressing the recombinant expanded ataxin-3 was observed at 20 and 26 days compared with *SCA3*-Q70 cells at 8 days (**$P < 0.01$, ***$P < 0.001$; ANOVA, followed by Tukey–Kramer multiple comparisons test). MTT reduction values are shown as OD values measured at a wavelength of 570 nm; each of the presented groups (Q23 and Q70) contains the results obtained from two individual isolated clonal cell lines and represent the means ± SD with $n = 10$.

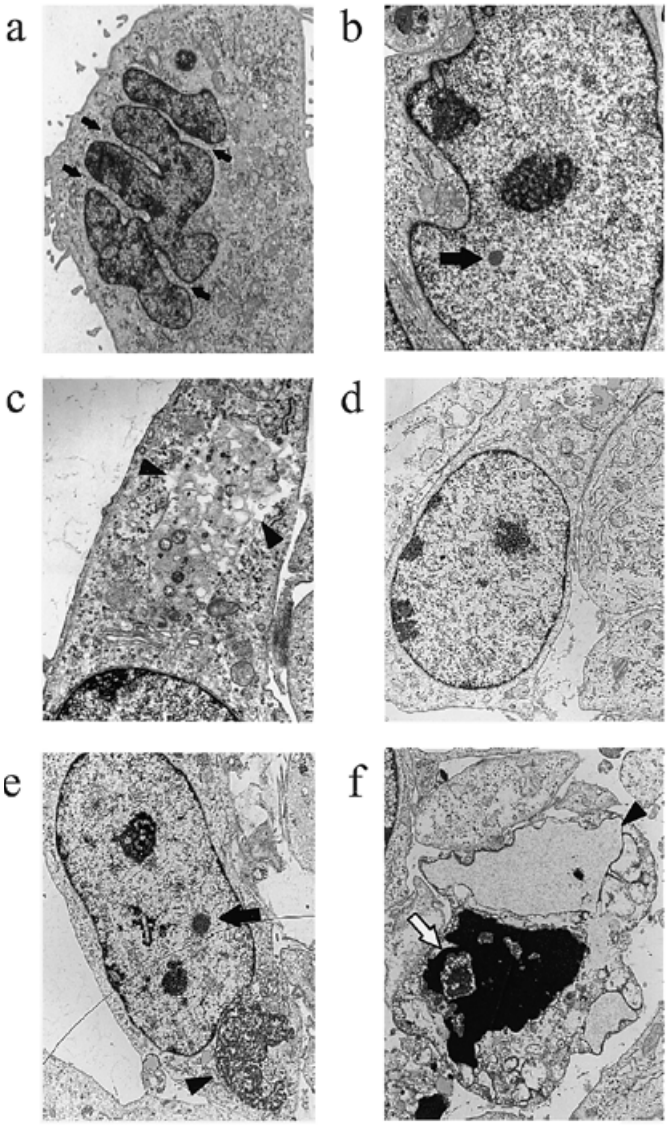

Figure 6. Electron microscopy analysis of clonal CSM14.1 cells stably expressing recombinant human full-length ataxin-3. Cells of transgenic lines were incubated for 3 or 20 days in the absence of tetracycline at 39°C and fixed for electron microscopy. Ultrastructural changes of CSM14.1 cells expressing expanded ataxin-3 (*SCA3*-Q70) for 3 days included (**a**) multiple indentations (arrows) of nuclei, (**b**) formation of nuclear bodies (arrow) and (**c**) strong cytoplasmic vacuolation (arrowheads). (**d**) Cells expressing non-expanded ataxin-3 (*SCA3*-Q23) showed normal appearance with oval shaped, euchromatin-rich nuclei, well-differentiated nucleoli and intact cytoplasm. Ultrastructural images of CSM14.1 cells expressing expanded ataxin-3 (*SCA3*-Q70) for 20 days additionally revealed (**e**) formation of large cytoplasmic (arrowhead) and nuclear inclusions (arrow) and (**f**) the presence of necrotic cells characterized by electron-dense chromatin deposits (white arrow), disintegrated mitochondria and extremely swollen endoplasmic reticulum profiles (arrowhead). Magnifications: (a) 3300×; (b) 6350×; (c) 10 500×; (d) 4800×; (e and f) 3810×.

Formation of intranuclear inclusions in cells expressing expanded ataxin-3

To investigate whether the observed spontaneous cell death of expanded ataxin-3-expressing cells coheres with time-dependent ultrastructural changes, cells of transgenic lines were incubated for 3 and 20 days in the absence of tetracycline at 39°C and analysed by electron microscopy. While cells from *SCA3*-Q23 cell lines (Fig. 6d) and the mock-transfected control cell line (data not shown) appeared normal, with intact and well-differentiated nuclei, the ultrastructure of nuclei of cells from *SCA3*-Q70 cell lines was characterized by strong indentations of the nuclear envelope, large disorganized nucleoli, strong segmentation of the nucleoli and intranuclear inclusions as early as 3 days after induced expression (Fig. 6a and b). The cytoplasm of these cells also revealed large membrane-bound vacuoles with remaining parts of organelles (Fig. 6c). These ultrastructural changes were still present after 20 days induced expression in *SCA3*-Q70 cell lines. Similarly, nuclei of most cells expressing expanded ataxin-3 were of irregular form and showed an increasing number of intranuclear bodies (data not shown). In addition, several of the cells expressing expanded ataxin-3 exhibited large cytoplasmic inclusions (Fig. 6e). However, we could not find morphological signs of apoptotic cell death by electron microscopy; instead dying cells of *SCA3*-Q70 cell lines exhibited signs of necrosis (Fig. 6f). They were characterized by extremely dilated endoplasmic reticulum

profiles and complete disintegration of organelles, including mitochondria and the Golgi complex. The chromatin structure within the nucleus was completely destroyed and consisted mainly of an electron-dense matrix, which was presumably formed from heterochromatin. None of these alterations was present in cells expressing non-expanded ataxin-3 or in cells of the mock-transfected control line (data not shown). Thus, cells with high level expression of the expanded form of ataxin-3 developed major morphological alterations resembling those found in affected neurons of SCA3 patients and exhibited non-apoptotic cell death.

Susceptibility of cell lines in response to an apoptotic stimulus

To determine whether the expression of an expanded ataxin-3 protein sensitizes neuronal cells to apoptotic cell death, the transgenic cell lines were exposed to staurosporine, a universal inducer of apoptosis, after 15 days of expression. Exposure to 1 μM staurosporine for 24, 48 and 72 h resulted in a continuous decrease in viable cells in all cell lines with greater vulnerability of neuronally differentiated cells at 39°C (data not shown). However, an increased vulnerability of cell lines expressing the expanded ataxin-3 protein in response to staurosporine was not evident. The staurosporine-induced cell death exhibited typical ultrastructural features of apoptosis in all isolated cell lines. Apoptotic cells were characterized by multiple nuclear fragments with marginal condensation of heterochromatin while untreated cells showed normal appearance (data not shown).

DISCUSSION

An increasing number of inherited neurodegenerative diseases are known to be caused by an expanded CAG trinucleotide repeat expansion. The molecular steps leading to a specific neuropathology induced by expanded polyglutamine-containing proteins are still unknown. Up to now, the mode of cell death is uncertain and controversial but may be associated with apoptotic mechanisms (28). We have developed a stable cellular model of SCA3 to investigate mechanisms of expanded ataxin-3-induced neurodegeneration. High level expression of a full-length human ataxin-3 with an expanded polyglutamine tract in the mesencephalic rat cell line CSM14.1 resulted in increased cell death starting 8 days after tetracycline withdrawal. Cell death specifically affected neuronally differentiated cells. In contrast, transient expression of full-length *SCA3* cDNA with 79 CAG repeats in monkey kidney COS-7 cells (14) or with 78 CAG repeats in human kidney 293T cells (15) failed to induce any cytotoxic effect. In these studies cytotoxicity was demonstrated only for truncated constructs containing a small portion of *SCA3* cDNA and the expanded CAG repeat. In contrast to the previous experiments, our system provides long-term expression and achieves high expression levels of the recombinant proteins. Consistent with our data, an increased susceptibility to cell death was reported for a tetracycline-inducible expression system of expanded full-length huntingtin in a neuroblastoma cell line (29).

CSM14.1 cell lines expressing expanded ataxin-3 accumulated the recombinant protein. Using the ataxin-3-specific monoclonal antibody 1H9, which specifically recognizes a 20 amino acid polypeptide upstream of the polyglutamine repeat (32), no proteolytic degradation of the disease protein was evident. However, immunodetection was restricted to protein fragments presenting this peptide sequence and further analyses with differentiating antibodies are required to investigate possible breakdown products. At present, pathogenicity in our cellular system seems to result from expressed expanded full-length ataxin-3 and does not appear to involve formation of toxic polyglutamine-containing fragments of the expanded ataxin-3 protein. It is interesting to note that in a recent report of SCA1 transgenic mice no correlation between the presence of detectable ataxin-1 cleavage products and the development of disease was found (33).

Thus far, formation of aggregates upon transient expression of expanded full-length ataxin-3 in COS-7, 293T or HeLa cells has been relatively poor and full-length ataxin-3 usually remains diffusely distributed in the cytoplasm of the transfected cells (14,15,34). Very recently, Chai *et al.* (34) demonstrated that addition of a nuclear localization signal to the N-terminus of an expanded full-length ataxin-3 resulted in nuclear redistribution and increased formation of intranuclear inclusions. In contrast, stable high level expression of the expanded human full-length ataxin-3 in CSM14.1 cells efficiently induced formation of intranuclear and cytoplasmic inclusions.

Immunocytochemical investigation of the subcellular distribution indicated that both non-expanded and expanded ataxin-3 variants were present in the nucleus. While this finding could represent an artefact from overexpression, a recent study found non-expanded ataxin-3 predominantly, but not exclusively, in the nucleus and associated with the inner nuclear matrix (35). Ataxin-3 might translocate to the nucleus without requirement of an elongated glutamine repeat via a nuclear localization signal (35). This is in contrast to the previously reported predominantly cytoplasmic staining of ataxin-3 in brains of unaffected individuals (12,13).

Ultrastuctural analysis of CSM14.1 cell lines expressing the expanded full-length ataxin-3 revealed strong indentations of the nuclear membrane and intranuclear inclusions. This parallels human SCA3 in which the most pronounced changes found in post-mortem sections of SCA3 disease brain are spherical intranuclear structures (15). The intranuclear inclusions induced by high level expression of expanded ataxin-3 in CSM14.1 cells were present several days before increased neuronal cell death was observed. Therefore, it is uncertain if the presence of these intranuclear inclusions was correlated with the observed spontaneous non-apoptotic cell death. Formation of intranuclear inclusions is characteristic of most polyglutamine-induced diseases although it is not clear whether generation of nuclear aggregates represents a protective or a degenerative mechanism for affected cells (36,37). Recently, transient transfection of full-length *HD* cDNA in primary striatal neurons was shown to result in formation of nuclear inclusions and induction of apoptotic cell death. In this study, the blocking of nuclear localization of mutant huntingtin led to inhibition of aggregation but also to a significant increase in cell death pointing towards a protective role of inclusions as part of a cellular defence strategy (28). More recently, co-localization of the 26S proteasome with polyglutamine aggregates was demonstrated in SCA3 tissue and three transiently transfected cell lines, providing evidence for involvement of the ubiquitin–proteasome pathway in SCA3 pathogenesis (34). Inhibitors of

the proteasome caused a repeat length-dependent increase in aggregate formation in HeLa and COS-7 cells without increasing the rate of cell death. Studies with SCA1 transgenic mice demonstrated that normal ataxin-1 localizes to several nuclear structures, whereas expanded ataxin-1 localizes to a single nuclear structure before the onset of ataxia (19). Transgenic mice expressing expanded ataxin-1 protein that contains a 122 amino acid deletion within the self-association region did not form nuclear aggregates but developed neurological symptoms of the disease (33). Thus, formation of aggregates is not necessarily a prerequisite for functional deficits and cell death. The altered nuclear distribution of expanded polyglutamine-containing proteins, however, seems to favour degenerative processes in neurons.

Furthermore, we found large membrane-bound cytoplasmic vacuoles and inclusions in cells expressing the expanded form of ataxin-3, reflecting additional morphological alterations which have also been reported for SCA1 transgenic Purkinje cells. In transgenic SCA1 mice, cytoplasmic vacuolation starts at 3 weeks of age and by 12 weeks of age is frequently accompanied by gliosis, thinning of the molecular layer and displacement of cell bodies from the Purkinje cell layer (38). In our *in vitro* model, the formation of intranuclear aggregates and vacuolation were present already after 3 days and proceeded until 20 days of induced expanded ataxin-3 expression. Formation of vacuoles may reflect a strong proteolytic activity of autophagosomes to protect cells from expanded ataxin-3-induced cytotoxicity. Autophagy is known to be an important way for a cell to get rid of obsolete parts, including aged or misfolded proteins from the cytoplasm (39).

The decreased viability of expanded ataxin-3-expressing cells after neuronal differentiation did not correlate with morphological signs of apoptosis; rather, cells expressing expanded ataxin-3 exhibited necrotic morphology by ultrastructural analysis. This is in contrast to a recent report where increased apoptotic cell death was observed in cells stably expressing expanded full-length huntingtin (29). In our model, cells overexpressing expanded ataxin-3 neither developed apoptotic morphology nor showed an increased susceptibility towards staurosporine-induced apoptosis. On the other hand, ultrastructural analysis of staurosporine-induced cell death demonstrated that the established cell lines were able to generate typical features of apoptosis.

We have presented a neuron-like cellular model for SCA3 where expression of an expanded full-length ataxin-3 resulted in increased spontaneous susceptibility to cell death, thereby reflecting important steps of human pathogenesis. This *in vitro* system should be useful as a model system for the investigation of the mechanisms involved in SCA3 pathogenesis and the assessment of possible therapeutic strategies.

MATERIALS AND METHODS

Plasmid construction

The *SCA3* cDNAs used for stable transfection encoded human full-length ataxin-3 with a normal repeat length of 23 units with the structure Q_3KQ_{19} (termed *SCA3*-Q23) or an expanded repeat with 70 units with the structure $Q_3KQ_{44}RQ_{21}$ (termed *SCA3*-Q70) and were originally isolated from brain cDNA libraries of a non-affected and an affected individual, respectively. The construction of the tetracycline-responsive plasmids was performed by cloning a blunted *Sac*II–*Not*I fragment containing the complete *SCA3*-Q23 cDNA and a blunted *Bam*HI–*Sal*I fragment containing the complete *SCA3*-Q70 cDNA in a blunted *Xba*I site of the pUHD10-3 response vector (31), generating the response plasmids pUHD-SCA3-Q23 and pUHD-SCA3-Q70. The generated response plasmids were verified by sequence analysis using an ABI 377 sequencer and contained completely identical 5'- and 3'-coding regions with the exception of the CAG repeat coding tract.

Generation of tetracycline-inducible stably transfected cell lines

All transfections in this study were performed by electroporation using a Bio-Rad (München, Germany) gene pulser (250 V, 950 μF). For the generation of the Tet-off response cell line 1×10^7 CSM14.1 cells were co-transfected with 20 μg of the regulator plasmid pUHD15-1 (31) and 2 μg of a selection marker (p65-hygro). Transfected cells were cultured in complete medium containing hygromycin (0.1 mg/ml) for 6–8 weeks. Individual hygromycin-resistent colonies were selected and characterized for their inducibility using transient transfections with the luciferase reporter plasmid pUHC13-3 (31). Luciferase activity was measured in the absence and presence of tetracycline (1 μg/ml) after 48–72 h transient expression with a luciferase assay system (Promega, Madison, WI) in a Berthold luminometer. The isolated Tet-off response CSM14.1 cell line with the highest tetracycline-responsive regulation was used for the second stable transfections with 25 μg of each of the *SCA3* constructs (pUHD-SCA3-Q23 and pUHD-SCA3-Q70) and the empty response plasmid pUHD10-3 (31), which served as a mock control, together with 5 μg of a second selection marker (pBABEpuro). Puromycin-resistent single cell colonies were isolated using puromycin (4 μg/ml) and tetracycline (1 μg/ml) in complete medium for 6–8 weeks. Individual double stable cell clones were characterized for transgene expression in the absence and presence of tetracycline (1 μg/ml) for 48–72 h by western blot analysis.

Western blot analysis

Soluble protein for western blotting was harvested from cells lysed for 15 min on ice in 50 mM Tris–HCl, pH 8.0, containing 120 mM NaCl, 5 mM EDTA, 0.5% NP-40, 2 μg/ml aprotinin, 100 μg/ml PMSF and 10 μg/ml leupeptin, followed by high speed centrifugation at 4°C. Supernatant was removed and protein concentration was determined using the Bradford assay (Bio-Rad). For electrophoresis, 20 μg protein aliquots were heat denatured by 5 min boiling in Laemmli loading buffer and separated by 10% SDS–PAGE and electroblotted to nitrocellulose membranes. Immunodetection involved blocking for 1 h in 10 mM Tris–HCl, pH 7.5, 150 mM NaCl, 5% skim milk (Difco, Detroit, MI), 2% BSA and 0.1% Tween 20, incubation with mAb 1H9 (1:5000 in blocking buffer) overnight at 4°C, incubation with peroxidase-coupled anti-mouse IgM [1:1000 in phosphate-buffered saline (PBS), 0.1% Tween 20] for 1 h at room temperature and detection using an ECL detection kit (Amersham, Braunscheig, Germany). The ataxin-3-specific mAb 1H9 recognizes a 20 amino acid polypeptide from E214 to L233 upstream of the glutamine tract (32).

Cell culture and neuronal differentiation

The rat mesencephalic dopaminergic CSM14.1 cell line (30) was cultured in Dulbecco's modified Eagle's medium (Gibco BRL, Eggenstein, Germany) supplemented with 10% heat-inactivated fetal calf serum, 100 U/ml penicillin and 100 µg/ml streptomycin, in a constant 5% CO_2 atmosphere either at the permissive temperature (33°C) or, for the purpose of neuronal differentiation, at the non-permissive temperature (39°C). For neuronal differentiation, cells were preincubated and allowed to attach overnight at 33°C and then switched to 39°C. After 7 days of culture at 39°C, cell growth arrested and >90% displayed neuron-like morphology characterized by neurite outgrowth. For western blot and electron microscopy analysis, cells were seeded at a density of 50 000 cells/ml in six-well plates. A density of 10 000 cells/ml was used for studies of cell proliferation and viability performed in 96-well microtitre plates as well as for immunocytochemistry performed on poly-L-lysine (0.01%)-coated eight-well chamber glass slides. In all experiments addressing effects of long-term expression of recombinant ataxin-3, the medium was changed every 5–7 days.

Assessment of cell proliferation and viability

Cell proliferation and viability were determined by the MTT (3-[4,5-dimethylthiazol-2-yl]-2,5-diphenyltetrazolium bromide) reduction assay. Cleavage of MTT by mitochondrial dehydrogenase enzymes yields a coloured formazan product only in metabolically active cells and has proved to be reliable for measurement of cell proliferation (40). The MTT reduction assay was performed by adding one tenth of an MTT (Sigma, Deisenhofen, Germany) stock solution in PBS (5 mg/ml) to the original culture volume and incubating cells for 2 h at the respective temperature. At the end of the incubation the medium was removed and the converted dye was solubilized with 100 µl DMSO. The absorbance of the converted dye was measured at 570 nm on a Dynatech (Dynex, Denkendorf, Germany) plate photometer.

Immunocytochemical detection of ataxin-3 expression

Cells were fixed in 4% paraformaldehyde and 1.5% glutaraldehyde in PBS (pH 7.4) for 10 min, washed in PBS and permeabilized in PBS containing 0.5% Triton X-100 for 5 min. After inactivation of the intrinsic peroxidase activity with 0.1% H_2O_2 for 10 min, the specimens were washed with PBS, blocked for 30 min with PBS containing 10% horse serum and incubated with the primary antibody mAb 1H9 (1:2000) for 1 h at room temperature. Following washes in PBS, the cells were incubated with peroxidase-conjugated anti-mouse IgG diluted 1:100 in PBS containing 5% horse serum. Detection was performed using diaminobenzidine as substrate.

Electron microscopy

For transmission electron microscopy, the cells were fixed for 1 h on ice in 0.05 M cacodylate buffer (pH 7.4) containing 2.5% glutaraldehyde and 0.08% paraformaldehyde, osmificated and embedded in Epon by standard procedures. Ultrathin sections were contrasted with uranyl acetate and lead citrate and examined with a Philips (Kassel, Germany) TEM 420 transmission electron microscope (41).

Statistics

Data are expressed as means ± SD. Statistical analysis was performed using one-way ANOVA followed by Tukey–Kramer multiple comparisons test (comparison of more than two groups). All experiments represent at least three independent replications performed with $n = 5$.

ACKNOWLEDGEMENTS

We thank Dr H. Bujard (Zentrum für Molekulare Biologie der Universität Heidelberg, Heidelberg, Germany) for the generous gift of the original plasmids of the Tet-off expression system, Dr M.F. Clarke (Departments of Medicine and Pathology, Ann Arbor, MI) for supplying the selection plasmid p65-hygro and Dr D.E. Bredesen (Burnham Institute, La Jolla, CA) for kindly providing the original rat mesencephalic dopaminergic CSM14.1 cell line. The excellent technical assistance of I. Müller and C. Kindermann is gratefully acknowledged. This work was supported by funds of the IKFZ (Interdisziplinäres Klinisches Forschungszentrum, Tübingen).

REFERENCES

1. Rosenberg, R.N. (1992) Machado–Joseph disease: an autosomal dominant motor system degeneration. *Mov. Disord.*, **7**, 193–203.
2. Takiyama, Y., Oyanagi, S., Kawashima, S., Sakamoto, H., Saito, K., Yoshida, M., Tsuji, S., Mizuno, Y. and Nishizawa, M. (1994) A clinical and pathologic study of a large Japanese family with Machado–Joseph disease tightly linked to the DNA markers on chromosome 14q. *Neurology*, **44**, 1302–1308.
3. Wellington, C.L., Brinkman, R.R., O'Kusky, J.R. and Harden, M.R. (1997) Toward understanding the molecular pathology of Huntington's disease. *Brain Pathol.*, **7**, 979–1002.
4. Kakizuka, A. (1997) Degenerative ataxias: genetics, pathogenesis and animal models. *Curr. Opin. Neurol.*, **10**, 285–290.
5. Robitaille, Y., Loppes-Cendes, I., Becher, M., Rouleau, G.A. and Clark, A.W. (1997) The neuropathology of CAG repeat diseases: review and update of genetic and molecular features. *Brain Pathol.*, **7**, 901–926.
6. Koshi, B.T. and Zoghbi, H.Y. (1997) The CAG/polyglutamine tract diseases: gene products and molecular pathogenesis. *Brain Pathol.*, **7**, 927–942.
7. Ross, A.C. (1997) Intranuclear neuronal inclusions: a common pathogenic mechanism for for glutamine-repeat neurodegenerative diseases? *Neuron*, **19**, 1147–1150.
8. David, G., Abbas, N., Stevanin, G., Dürr, A., Yvert, G., Cancel, G., Weber, C., Imbert, G., Saudou, F., Antoniou, E., Drabkin, H., Gemmill, R., Giunti, P., Benomar, A., Wood, N., Ruberg, M., Agid, Y., Mandel, J.L. and Brice, A. (1997) Cloning of the *SCA7* gene reveals a highly unstable CAG repeat expansion. *Nature Genet.*, **17**, 65–70.
9. Kawaguchi, Y., Okamoto, T., Taniwaki, M., Aizawa, M., Inoue, M., Katayama, H., Nakamura, S., Nishimura, M., Akiguchi, I., Kimura, J., Narumiya, S. and Kakizuka, A. (1994) CAG expansions in a novel gene for Machado–Joseph disease at chromosome 14q32.1. *Nature Genet.*, **8**, 221–227.
10. Dürr, A., Stevanin, G., Cancel, G., Duyckaerts, C., Abbas, N., Didierjean, O., Chneiweiss, H., Benomar, A., Lyon-Caen, O., Julien, J., Serdaru, M., Penet, C., Agid, Y. and Brice, A. (1996) Spinocerebellar ataxia 3 and Machado–Joseph disease: clinical, molecular and neuropathological features. *Ann. Neurol.*, **39**, 490–499.
11. Trottier, Y., Lutz, Y., Stevanin, G., Imbert, G., Devys, D., Cancel, G., Saudou, F., Weber, C., David, G., Tora, L., Agid, Y., Brice, A. and Mandel, J.L. (1995) Polyglutamine expansion as a pathological epitope in Huntington's disease and four dominant cerebellar ataxias. *Nature*, **378**, 403–406.
12. Paulson, H.L., Das, S.S., Crino, P.B., Perez, M.K., Patel, S.C., Gotsdiner, D., Fischbeck, K.H. and Pittman, R.N. (1997) Machado–Joseph disease gene product is a cytoplasmic protein widely expressed in brain. *Ann. Neurol.*, **41**, 453–462.
13. Schmidt, T., Landwehrmeyer, G.B., Schmitt, I., Trottier, Y., Auburger, G., Laccone, F., Klockgether, T., Völpel, M., Epplen, J.T., Schöls, L. and Riess, O. (1998) An isoform of ataxin-3 accumulates in the nucleus of neuronal cells in affected brain regions of SCA3 patients. *Brain Pathol.*, **8**, 669–679.

14. Ikeda, H., Yamaguchi, M., Sugai, S., Aze, Y., Narumiya, S. and Kakizuka, A. (1996) Expanded polyglutamine in the Machado–Joseph disease protein induces cell death *in vitro* and *in vivo*. *Nature Genet.*, **13**, 196–202.
15. Paulson, H.L., Perez, M.K., Trottier, Y., Trojanowski, J.Q., Subramony, S.H., Das, S.S., Vig, P., Mandel, J.L., Fischbeck, K.H. and Pittman R.N. (1997) Intranuclear inclusions of expanded polyglutamine protein in spinocerebellar ataxia type 3. *Neuron*, **19**, 333–344.
16. Davies, S.W., Turmaine, M., Cozens, B.A., DiFiglia, M., Sharp, A.H., Ross, C.A., Scherzinger, E., Wanker, E.E., Mangiarini, L. and Bates, G.P. (1997) Formation of neuronal intranuclear inclusions underlies the neurological dysfunction in mice transgenic for the HD mutation. *Cell*, **90**, 537–548.
17. Scherzinger, E., Lurz, R., Turmaine, M., Mangiarini, L., Hollenbach, B., Hasenbank, R., Bates, G.B., Davies, S.W., Lehrach, H. and Wanker, E.E. (1997) Huntingtin-encoded polyglutamine expansions form amyloid-like protein aggregates *in vitro* and *in vivo*. *Cell*, **90**, 549–558.
18. DiFiglia, M., Sapp, E., Chase, K.O., Davies, S.W., Bates, G.P., Vonsattel, J.P. and Aronin, N. (1997) Aggregation of huntingtin in neuronal intranuclear inclusions and dystrophic neurites in brain. *Science*, **277**, 1990–1993.
19. Skinner, P.J., Koshy, B.T., Cummings, C.J., Klement, I.A., Helin, K., Servadio, A., Zoghbi, H.Y. and Orr, H.T. (1997) Ataxin-1 with an expanded glutamine tract alters nuclear matrix-associated structures. *Nature*, **389**, 971–974.
20. Matilla, A., Koshy, B.T., Cummings, C.J., Isobe, T., Orr, H.T. and Zoghbi, H.Y. (1997) The cerebellar leucine-rich acidic nuclear protein interacts with ataxin-1. *Nature*, **389**, 974–978.
21. Klockgether, T. and Evert, B. (1998) Genes involved in hereditary ataxias. *Trends Neurosci.*, **21**, 413–418.
22. Mangiarini, L., Sathasivam, K., Seller, M., Cozens, B., Harper, A., Hetherington, C., Lawton, M., Trottier, Y., Lehrach, H., Davies, S.W. and Bates, G.P. (1996) Exon 1 of the HD gene with an expanded CAG repeat is sufficient to cause a progressive neurological phenotype in transgenic mice. *Cell*, **87**, 493–506.
23. Burright, E.N., Clark, H.B., Servadio, A., Matilla, T., Feddersen, R.M., Yunis, W.S., Duvick, L.A., Zoghbi, H.Y. and Orr, H.T. (1995) SCA1 transgenic mice: a model for neurodegeneration caused by an expanded CAG trinucleotide repeat. *Cell*, **82**, 937–948.
24. Ordway, J.M., Tallaksen-Greene, S., Gutekunst, C.A., Bernstein, E.M., Cearley, J.A., Wiener, H.W., Dure, L.S.IV, Lindsey, R., Hersch, S.M., Jope, R.S., Albin, R.L. and Detloff, P.J. (1997) Ectopically expressed CAG repeats cause intranuclear inclusions and a progressive late onset neurological phenotype in the mouse. *Cell*, **91**, 753–763.
25. Warrick, J.M., Paulson, H.L., Gray-Board, G.L., Bui, Q.T., Fischbeck, K.H., Pittman, R.N. and Bonini, N.M. (1998) Expanded polyglutamine protein forms nuclear inclusions and causes neural degeneration in *Drosophila*. *Cell*, **93**, 939–949.
26. Reddy, P.H., Williams, M., Charles, V., Garrett, L., Pike-Buchanan, L., Whetsell, W.O., Miller, G. and Tagle, D.A. (1998) Behavioural abnormalities and selective neuronal loss in HD transgenic mice expressing mutated full-length HD cDNA. *Nature Genet.*, **20**, 198–202.
27. Martindale, D., Hackam, A., Wieczorek, A., Ellerby, L., Wellington, C., McCutcheon, K., Singaraja, R., Kazemi-Esfarjani, P., Devon, R., Kim, S.U., Bredesen, D.E., Tufaro, F. and Hayden, M.R. (1998) Length of huntingtin and its polyglutamine tract influences localization and frequency of intracellular aggregates. *Nature Genet.*, **18**, 150–154.
28. Saudou, F., Finkbeiner, S., Devys, D. and Greenberg, M.E. (1998) Huntingtin acts in the nucleus to induce apoptosis but death does not correlate with the formation of intranuclear inclusions. *Cell*, **95**, 55–66.
29. Lunkes, A. and Mandel, J.L. (1998) A cellular model that recapitulates major pathogenic steps of Huntington's disease. *Hum. Mol. Genet.*, **7**, 1355–1361.
30. Durand, M.M., Chugani D.C., Mahmoudi, M. and Phelps, M.E. (1990) Characterization of neuron-like cell line immortalized from primary rat mesencephalon cultures. *Neurosci. Abstr.*, **16**, 40.
31. Gossen, M. and Bujard, H. (1992) Tight control of gene expression in mammalian cells by tetracycline-responsive promoters. *Proc. Natl Acad. Sci. USA*, **89**, 5547–5551.
32. Trottier, Y., Cancel, G., An-Gourfinkel, I., Lutz, Y., Weber, C., Brice, A., Hirsch, E. and Mandel, J.L. (1998) Heterogenous intracellular localization and expression of ataxin-3. *Neurobiol. Dis.*, **5**, 335–347.
33. Klement, I.A., Skinner, P.J., Kaytor, M.D., Yi, H., Hersch, S.M., Clark, H.B., Zoghbi, H.Y. and Orr, H.T. (1998) Ataxin-1 localization and aggregation: role in polyglutamine-induced disease in SCA1 transgenic mice. *Cell*, **95**, 41–53.
34. Chai, Y., Koppenhafer, S.L., Shoesmith, S.J., Perez, M.K. and Paulson, H.L. (1999) Evidence for proteasome involvement in polyglutamine disease: localization to nuclear inclusions in SCA3/MJD and suppression of polyglutamine aggregation *in vitro*. *Hum. Mol. Genet.*, **8**, 673–682.
35. Tait, D., Riccio, M., Sittler, A., Scherzinger, E., Santi, S., Ognibene, A., Maraldi, N.M., Lehrach, H. and Wanker, E.E. (1998) Ataxin-3 is transported into the nucleus and associates with the nuclear matrix. *Hum. Mol. Genet.*, **7**, 991–997.
36. Sisodia, S.S. (1998) Nuclear inclusions in glutamine repeat disorders: are they pernicious, coincidental, or beneficial? *Cell*, **95**, 1–4.
37. Kim, T.W. and Tanzi, R.E. (1998) Neuronal intranuclear inclusions in polyglutamine diseases: nuclear weapons or nuclear fallout? *Neuron*, **21**, 657–659.
38. Clark, H.B., Burright, E.N., Yunis, W.S., Larson, S., Wilcox, C., Hartman, B., Matilla, A., Zoghbi, H.Y. and Orr, H.T. (1997) Purkinje cell expression of a mutant allele of SCA1 in transgenic mice leads to disperate effects on motor behaviors, followed by a progressive cerebellar dysfunction and histological alterations. *J. Neurosci.*, **17**, 7385–7395.
39. Jentsch, S. and Ulrich, H.D. (1998) Ubiquitous déjà vu. *Nature*, **395**, 321–323.
40. Mosmann, T. (1983) Rapid colorimetric assay for cellular growth and survival: application to proliferation and cytotoxicity assays. *J. Immunol. Methods*, **65**, 55–63.
41. Kressel, M. and Groscurth, P. (1994) Distinction of apoptotic and necrotic cell death by *in situ* labelling of fragmented DNA. *Cell Tissue Res.*, **278**, 549–556.